Supporting Information

Lightweight Free-Standing CeF_3 Nanorod/Carbon Nanotube Composite Interlayer for Lithium-Sulfur Batteries

Kunyang Zou [a], Na Li [b], Yuanzhen Chen [a,*], Xin Dai [a], Weitao Jing [a], Ming Shi [a], Chenjie Lu [c], Qiang Tan [a], Yanfei Xin [a], Junjie Sun [a], Yongning Liu [a,*]

[a] State Key Laboratory for Mechanical Behavior of Materials, School of Material Science and Engineering, Xi'an Jiaotong University, Xi'an 710049, PR China

[b] Research I Department, ABM (Factory), Division 2, Battery Business Group BYD Lithium Battery Co, Ltd, Shenzhen, 518116, PR China

[c] MOE Key Laboratory of Macromolecular Synthesis and Functionalization, and Key Laboratory of Adsorption and Separation, Materials & Technologies of Zhejiang Province, Department of Polymer Science & Engineering, Zhejiang University, Hangzhou 310027, China

E-mail addresses: cyz1984@xjtu.edu.cn (Y.Chen), ynliu@xjtu.edu.cn (Y.Liu)

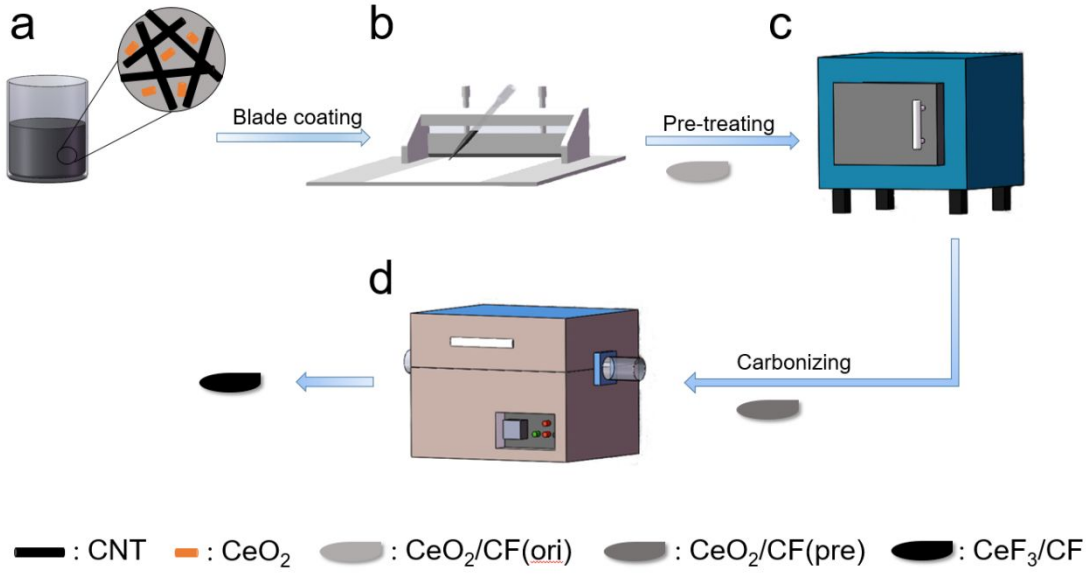

Figure. S1. Preparation processes of CeO_2/CF(ori), CeO_2/CF(pre), CeF_3/CF membrane. (a) slurry of CNT/CeO_2/PVDF, (b) blade coating slurry to obtain CeO_2/CF(ori), (c) obtain CeO_2/CF(pre) through Pre-treating, (d) obtain CeF_3/CF through Carbonizing.

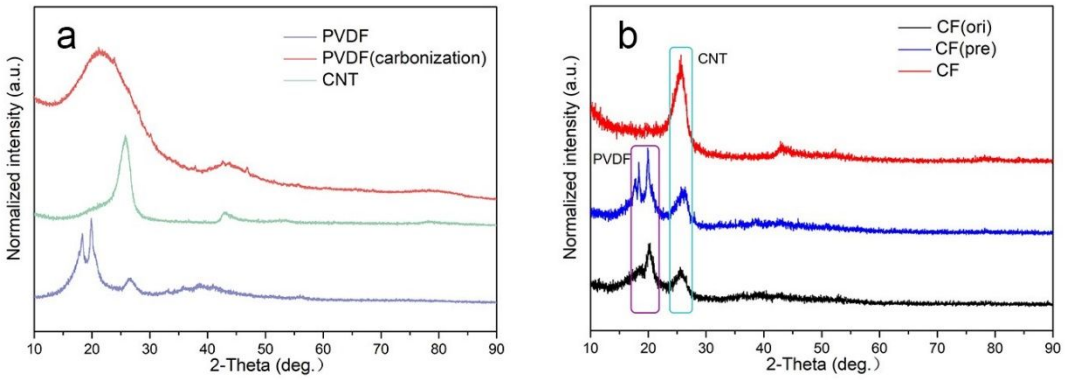

Figure. S2. XRD patterns of (a) PVDF, PVDF(carbonization), CNT, (b) XRD patterns of CF(ori), CF(pre), CF.

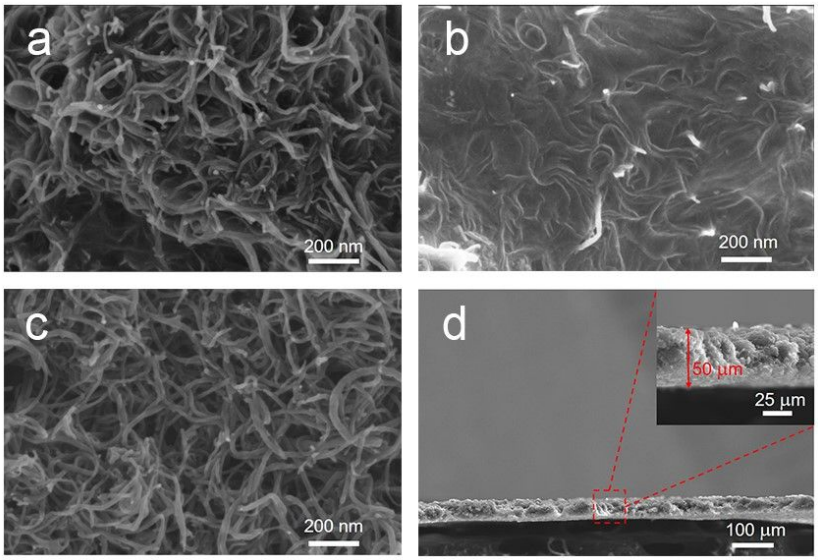

Figure. S3. SEM images of (a) CF(ori), (b) CF(pre), (c) CF, (d) CeF_3-20/CF.

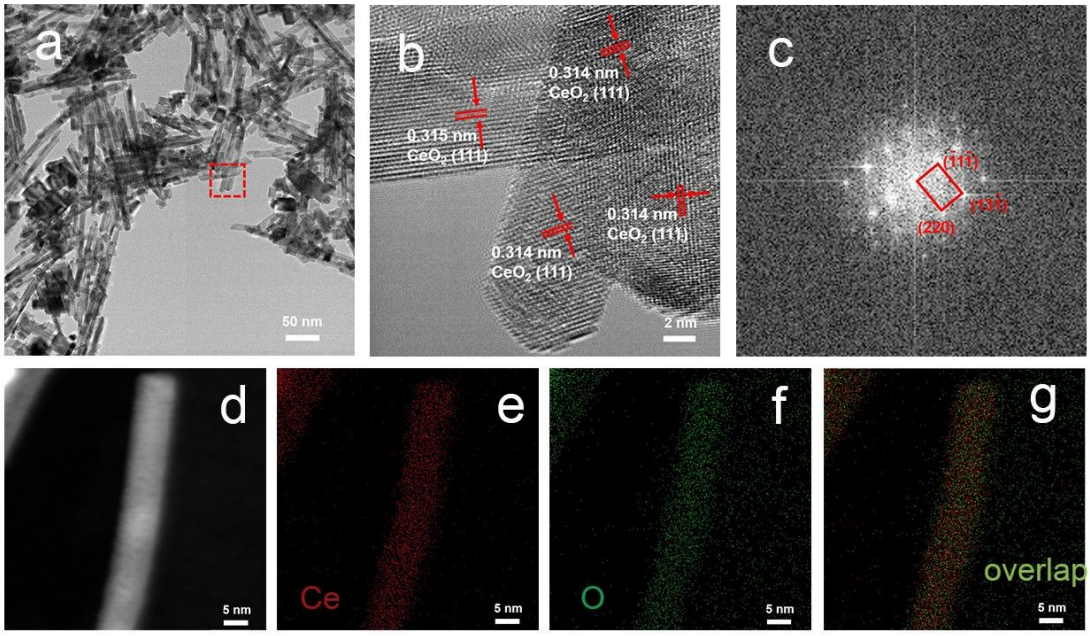

Figure. S4. Structure and morphological characterization of nanorod-like CeO_2: (a) STEM image, (b) HRTEM image, (c) FFT pattern, (d) STEM image and its corresponding EDS elemental mapping images: (e) Ce, (f) O, (g) image of overlap.

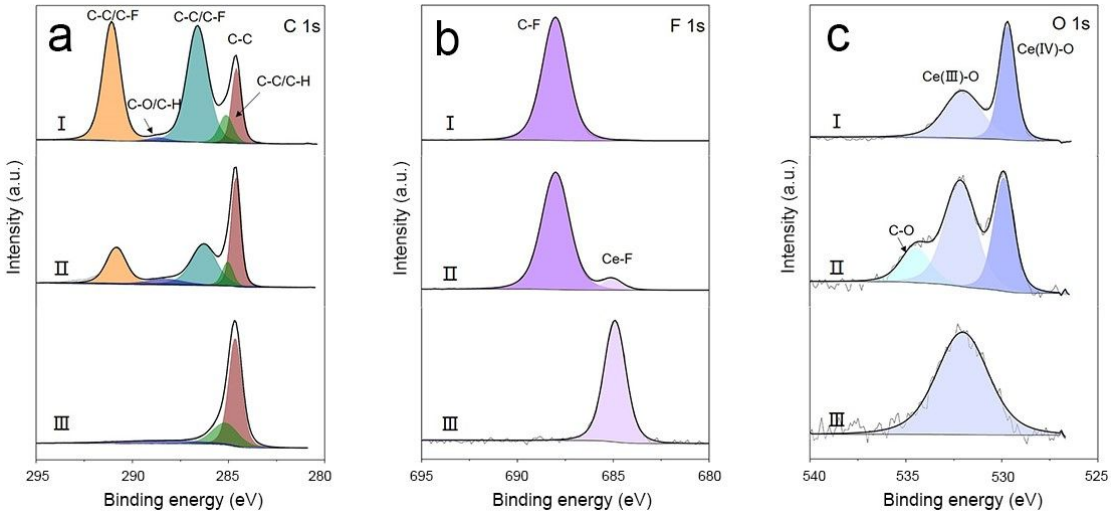

Figure. S5. XPS spectra and of CeO_2-20/CF(ori), CeO_2-20/CF (pre), CeF_3-20/CF: (a) C 1s XPS spectra, (b) F 1s XPS spectra, (c) O 1s XPS spectra.

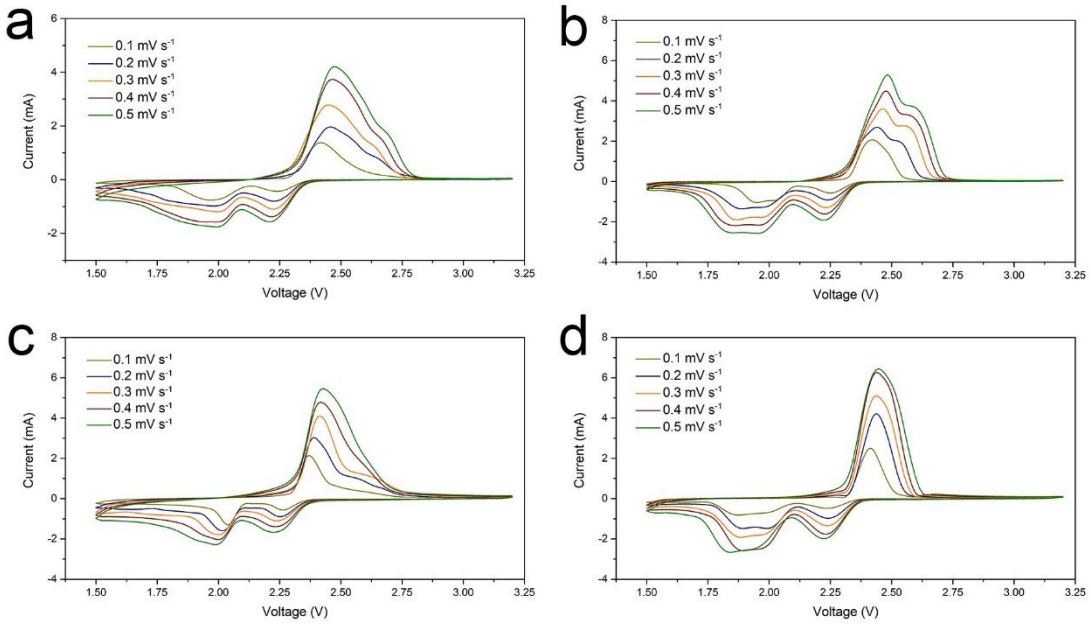

Figure. S6. Typical cyclic voltammetry (CV) profile of (a) CF(ori), (b) CF(pre), (c) CF and (d) CeF_3-20/CF under different scan rate from 0.1 mV s^{-1} to 0.5 mV s^{-1}.

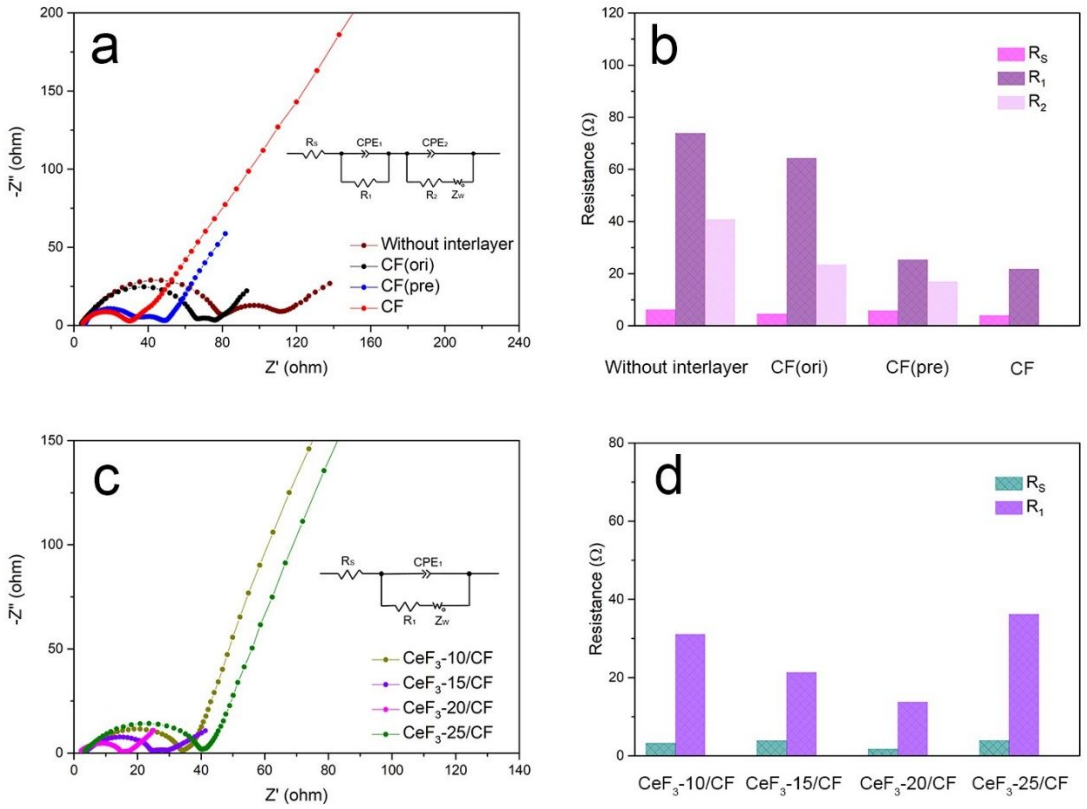

Figure. S7. The EIS of the lithium sulfur batteries: (a) Nyquist plots of the batteries with the CF(ori), CF(pre), CF interlayers, and no interlayer after first cycle, (b) the corresponding resistance of the batteries of (a), (c) Nyquist plots of the batteries based on the CeF_3-10/CF, CeF_3-15/CF, CeF_3-20/CF, and CeF_3-25/CF interlayers after first cycle, (d) the corresponding resistance of the batteries of (a).

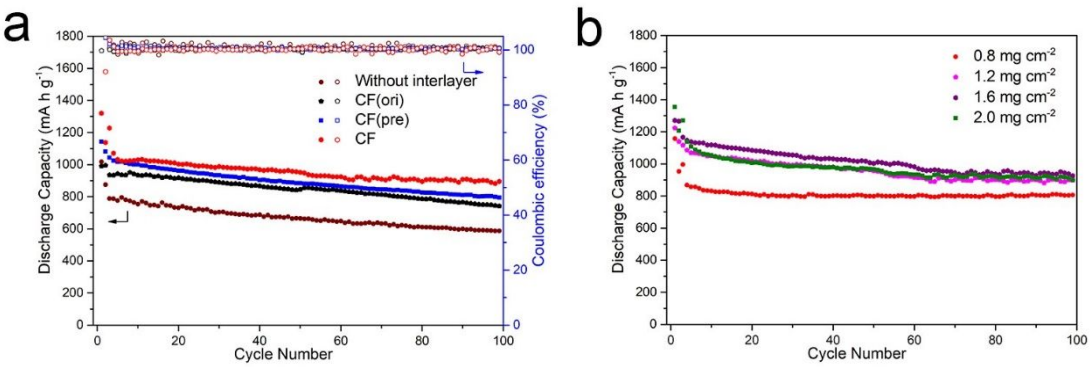

Figure. S8. Electrochemical performances of samples as interlayers: (a) battery cycling performance of no film, CF(ori), CF(pre) and CF film at 0.2C, (b) cycle performance of batteries with CeF_3-20/CF of different mass per unit area.

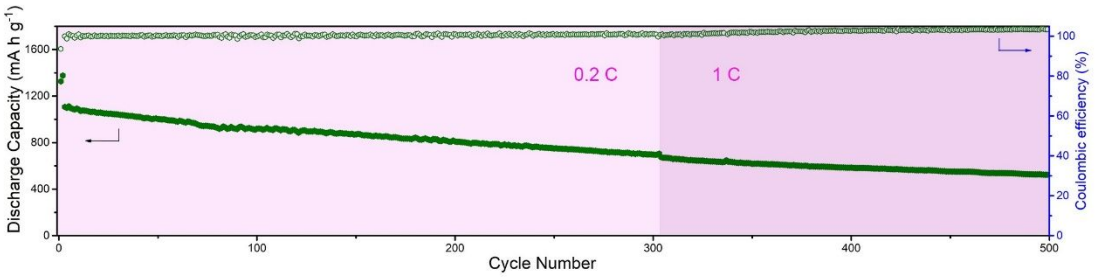

Figure. S9. Long cycle performance of the battery with CeF_3-20/CF under the rate of 0.2 C and 1 C.

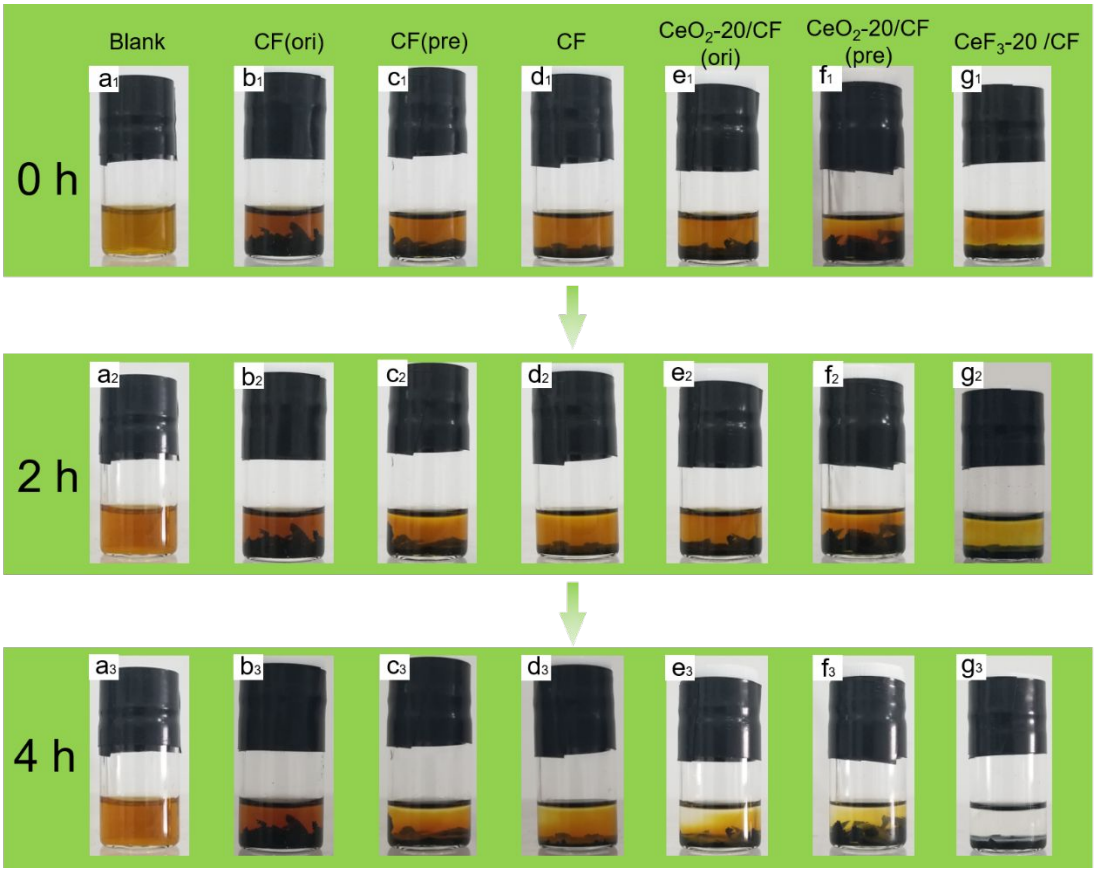

Figure. S10. Visualized adsorption of Li_2S_4 on CF(ori), CF(pre), CF, CeO_2-20/CF(ori), CeO_2-20/CF(pre) and CeF_3-20/CF with the same mass.

Table S1. Comparison of the mass loss of PVDF before and after carbonization.

	First	Second	Third	Average value
Before (g)	1	1	1	1
After (g)	0.351	0.349	0.351	0.3503
The mass loss ratio (%)	64.9%	65.1%	64.9%	64.97%

Table S2

Comparison of electrochemical performance of Li-S batteries with different interlayers/functional separators.

Materials	Preparation method	Base structure	Interlayer/ Functional separator	Discharge current rate(mA g^{-1})	Initial discharge capacity / Residual reversible capacity(mAh g^{-1})	Degradation rate per cycle	Reference
Carbon/CNT/ CeF_3	**Slurry casting /Carbonization**	**No**	**Interlayer**	**435**	**1015/951**	**0.063% for 100 cycles**	**This Work**
CNT-loaded GF composite paper	Sonication	GF paper	Interlayer	-	1111/802	0.12% for 230 cycles	1
Fe_3C/CNF	Electrospinning	No	Interlayer	200	1177/893	0.24% for 100 cycles	2
MCM-41/MWCNT-PEI nanofiber on PAN+Al_2O_3	Electrospinning	No	Interlayer	921	900/600	0.222% for 150 cycles	3
PAN-GO	Electrospinning	No	Interlayer	335	963/597	0.38% for 100 cycles	4
RGO-PVDF	Electrospinning	No	Interlayer	368	1100/647	0.206% for 200 cycles	5
Nickel foam	-	Nickel foam	Interlayer	336	820/604	0.33% for 80 cycles	6
GO/Cellulose	Vacuum filtration	Cellulose	Interlayer	300	2736/474	0.42% for 200 cycles	7
GO/Carbon black	Vacuum filtration	No	Interlayer	168	1260/894	0.29% for 100 cycles	8

Carbon fiber monolith	Vacuum filtration	No	Interlayer	336	1120/630	0.44% for 100 cycles	9
Acetylene black/PTFE	Thermal decomposition	No	Interlayer	168	1491/1062	0.58% for 50 cycles	10
Carbon paper	-	Carbon paper	Interlayer	336	1500/810	0.92% for 50 cycles	11
GO/CNT	Vacuum filtration	No	Interlayer	336	1370/671	0.17% for 300 cycles	12
Super P/Glass fiber	Slurry casting	PP film	Functional separator	234	1350/851	0.185% for 200 cycles	13
SiO_2 nanoparticle	Dip coating	PP film	Functional separator	469	937/604	0.178% for 200 cycles	14
Microporous carbon/Glass fiber	Physical contact	PP film	Functional separator	515	1166/700	0.2% for 200 cycles	15
Poly(styrenesulfonate)(PSS)	Dip coating	PP film	Functional separator	837	1070/719	0.82% for 40 cycles	16
Boron-rGO	Slurry casting	PP film	Functional separator	261	1227/664	0.153% for 300 cycles	17

References

(1) Lee, C.-L.; Kim, I.-D. A Hierarchical Carbon Nanotube-Loaded Glass-Filter Composite Paper Interlayer with Outstanding Electrolyte uptake Properties for High-Performance Lithium–Sulphur Batteries. *Nanoscale* **2015,** *7* (23), 10362-10367.

(2) Huang, J.-Q.; Zhang, B.; Xu, Z.-L.; Abouali, S.; Akbari Garakani, M.; Huang, J.; Kim, J.-K. Novel Interlayer Made from Fe3C/Carbon Nanofiber Webs for High Performance Lithium–Sulfur Batteries. *Journal of Power Sources* **2015,** *285*, 43-50.

(3) Kim, J.-H.; Jung, G. Y.; Lee, Y.-H.; Kim, J.-H.; Lee, S.-Y.; Kwak, S. K.; Lee, S.-Y. Polysulfide-Breathing/Dual-Conductive, Heterolayered Battery Separator Membranes Based on 0D/1D Mingled Nanomaterial Composite Mats. *Nano Letters* **2017,** *17* (4), 2220-2228.

(4) Zhu, J.; Chen, C.; Lu, Y.; Zang, J.; Jiang, M.; Kim, D.; Zhang, X. Highly Porous Polyacrylonitrile/Graphene Oxide Membrane Separator Exhibiting Excellent Anti-Self-Discharge Feature for High-Performance Lithium–Sulfur Batteries. *Carbon* **2016,** *101*, 272-280.

(5) Zhu, P.; Zhu, J.; Zang, J.; Chen, C.; Lu, Y.; Jiang, M.; Yan, C.; Dirican, M.; Kalai Selvan, R.; Zhang, X. A Novel Bi-Functional Double-Layer rGO–PVDF/PVDF Composite Nanofiber Membrane Separator with Enhanced Thermal Stability and Effective Polysulfide Inhibition for High-Performance Lithium–Sulfur Batteries. *Journal of Materials Chemistry A* **2017,** *5* (29), 15096-15104.

(6) Zhang, K.; Qin, F.; Fang, J.; Li, Q.; Jia, M.; Lai, Y.; Zhang, Z.; Li, J. Nickel Foam as Interlayer to Improve the Performance of Lithium–Sulfur Battery. *Journal of Solid State Electrochemistry* **2014,** *18* (4), 1025-1029.

(7) Leng, X.; Wu, K.-H.; Gentle, I. R.; Wang, D.-W. Electroactive Cellulose-Supported Graphene Oxide Interlayers for Li–S Batteries. *Carbon* **2015,** *93*, 611-619.
(8) Wang, X.; Wang, Z.; Chen, L. Reduced Graphene Oxide Film as a Shuttle-Inhibiting Interlayer in a Lithium–Sulfur Battery. *Journal of Power Sources* **2013,** *242*, 65-69.
(9) Zhang, L.; Wang, Y.; Peng, B.; Yu, W.; Wang, H.; Wang, T.; Deng, B.; Chai, L.; Zhang, K.; Wang, J. Preparation of a Macroscopic, Robust Carbon-Fiber Monolith from Filamentous Fungi and its Application in Li–S Batteries. *Green Chemistry* **2014,** *16* (8), 3926-3934.
(10) Jeong, T.-G.; Moon, Y. H.; Chun, H.-H.; Kim, H. S.; Cho, B. W.; Kim, Y.-T. Free Standing Acetylene Black Mesh to Capture Dissolved Polysulfide in Lithium Sulfur Batteries. *Chemical Communications* **2013,** *49* (94), 11107-11109.
(11) Zhang, K.; Li, Q.; Zhang, L.; Fang, J.; Li, J.; Qin, F.; Zhang, Z.; Lai, Y. From Filter Paper to Carbon Paper and Toward Li–S Battery Interlayer. *Materials Letters* **2014,** *121*, 198-201.
(12) Huang, J.-Q.; Xu, Z.-L.; Abouali, S.; Akbari Garakani, M.; Kim, J.-K. Porous Graphene Oxide/Carbon Nanotube Hybrid Films as Interlayer for Lithium-Sulfur Batteries. *Carbon* **2016,** *99*, 624-632.
(13) Zhu, J.; Ge, Y.; Kim, D.; Lu, Y.; Chen, C.; Jiang, M.; Zhang, X. A Novel Separator Coated by Carbon for Achieving Exceptional High Performance Lithium-Sulfur Batteries. *Nano Energy* **2016,** *20*, 176-184.
(14) Li, J.; Huang, Y.; Zhang, S.; Jia, W.; Wang, X.; Guo, Y.; Jia, D.; Wang, L. Decoration of Silica Nanoparticles on Polypropylene Separator for Lithium–Sulfur Batteries. *ACS Applied Materials & Interfaces* **2017,** *9* (8), 7499-7504.
(15) Wang, L.; Liu, J.; Haller, S.; Wang, Y.; Xia, Y. A Scalable Hybrid Separator for a High Performance Lithium–Sulfur Battery. *Chemical Communications* **2015,** *51* (32), 6996-6999.
(16) Conder, J.; Forner-Cuenca, A.; Gubler, E. M.; Gubler, L.; Novák, P.; Trabesinger, S. Performance-Enhancing Asymmetric Separator for Lithium–Sulfur Batteries. *ACS Applied Materials & Interfaces* **2016,** *8* (29), 18822-18831.
(17) Wu, F.; Qian, J.; Chen, R.; Ye, Y.; Sun, Z.; Xing, Y.; Li, L. Light-Weight Functional Layer on a Separator as a Polysulfide Immobilizer to Enhance Cycling Stability for Lithium–Sulfur Batteries. *Journal of Materials Chemistry A* **2016,** *4* (43), 17033-17041.